Università degli Studi di Padova

Dipartimento di Fisica e Astronomia " G. Galilei "
Corso di laurea in Fisica

Tesi di Laurea

Dissipative effects in the dynamics of a Bose-Einstein condensate under double-well confinement

Relatore:
Prof. Luca Salasnich

Laureando:
Antonio Tiene
Matricola: 1073890

Anno Accademico 2015/2016

Università degli Studi di Padova

Dipartimento di Fisica e Astronomia " G. Galilei "
Corso di laurea in Fisica

Tesi di Laurea

Dissipative effects in the dynamics of a Bose-Einstein condensate under double-well confinement

Relatore:
Prof. Luca Salasnich: .....

Laureando:
Antonio Tiene: .....
Matricola: 1073890

Contents

Introduction

The coupling of two macroscopic quantum states through a tunnel barrier brings to Josephson phenomena such as Rabi oscillations, the AC and DC effects, or macroscopic self-trapping, depending on whether tunnelling or interactions dominate. This effects were seen for the first time by the British physicist Brian Josephson, and one way to obtain them theoretically is using the Gross–Pitaevskii equation (named after Eugene Gross and Lev Pitaevskii), that describes the ground state of a quantum system of identical bosons using the Hartree–Fock approximation and the pseudopotential interaction model. The aim of this work is to analyze the general behavior of a Bose-Einstein condensate under a double-well confinement and to describe what happens with the introduction of a dissipative term in the Gross-Pitaevskii equation. In particular we are interested in the dynamics of the systems and how the transition between Josephson regime and self-trapping regime changes in a dissipative system.
In chapter 1 we describe the concepts of Bose-Einstein condensate and ultracold atoms, using the Gross–Pitaevskii equation and its dimensional reduction to 1-D GPE.
In chapter 2 we analyze the dynamics of a Bose-Einstein condensation analytically, getting the Josephson equation from the 1-D GPE, and numerically, using the four-order Runge-Kutta method, that helps us to understand the time evolution of the system.
In chapter 3 we perform analytical and numerical analysis of a dissipative coupled system, obtained simply adding a dissipative term in the GPE.
Chapter 4 is a brief check of our results with a seminal experimental evidence in the study of coupled macroscopic quantum states.

Chapter 1

Ultracold atoms and Bose-Einstein condensation

Ultracold atoms are atoms that are maintained at temperatures close to 0 kelvin (absolute zero), typically below temperatures of some tenths of microkelvins (μK). At these temperatures the atom's quantum-mechanical properties become important.
The study of ultracold atoms is important for understanding Bose-Einstein condensation (BEC), bosonic superfluidity, quantum magnetism, Bardeen-Cooper-Schrieffer (BCS) superfluidity and the BEC-BCS crossover.

In particular, the study of BEC is one of the most important field of physics. Theorized by A. Einstein and S.M. Bose [1, 2] in 1925, a Bose-Einstein condensation is a particular condition in which, taking an ideal Bose gas at zero temperature, all particles occupy the lowest energy level. So all particles are in the same single-particle quantum state.
The first experimental evidence was the observation of a BEC in 1995 [3], using alkali-metal atoms confined and cooled down to a temperature of 100 nK.

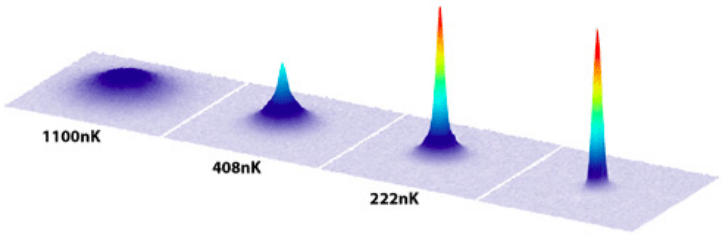

Figure 1.1: BEC of Erbium. Obtained by Ferlaino group, Innsbruck in 2012.

Mathematically, for a couple of bosons, the wave function is odd respect to swapping particles

$$\Psi_{n_1,n_2}(\vec{x}_1,\vec{x}_2) = \frac{1}{\sqrt{2}}(\Psi_{n_1}(\vec{x}_1)\Psi_{n_2}(\vec{x}_2) + \Psi_{n_1}(\vec{x}_2)\Psi_{n_2}(\vec{x}_1)).$$

Generalizing to the N dimensional case

$$\Psi_n(\vec{x}_1,...,\vec{x}_n) = \frac{1}{\sqrt{N!}}\frac{1}{\prod_n \sqrt{v_n!}}\sum_Q(\Psi_{n_1}(Q\vec{x}_1))...(\Psi_{n_n}(Q\vec{x}_n)),$$

with Q the possible permutation, and v_n the occupation number of the state n.
To describe an ideal Bose gas at finite temperature, we can use the Bose-Einstein distribution $N_\alpha = \frac{g_\alpha}{e^{\beta(\epsilon_\alpha-\mu)-1}}$, with N_α the number of bosons in the state $|\alpha\rangle$ of energy ϵ_α, $\mu < \epsilon_0$ the chemical potential, β the Bose thermal distribution an g_α the degeneration of the state $|\alpha\rangle$. It is useful to introduce the concept of BEC fraction $\frac{N_0}{N} = 1 - \frac{\sum N_\alpha}{N}$, and of critical temperature. The latter one is the temperature at which the number of condensated bosons starts to increase, the fugacity is equal to 1, and consequently the chemical potential is 0.
A theoretical description of BEC at $T = 0°K$ is given by the use of Gross-Pitaevskii equation (GPE).Taking a system composed by N bosons, with an external potential U($\vec{r}_i$) and an interacting potential $V(\vec{r}_i, \vec{r}_j)$, the N-body hamiltonian is

$$\widehat{H} = \sum_{i=1}^{N} (-\frac{\hbar^2}{2m}\nabla_i^2 + U(\vec{r}_i)) + \frac{1}{2}\sum_{ij=1}^{N} V(\vec{r}_i, \vec{r}_j).$$

We said above that a BEC is a collection of bosons in the fundamental state. The ground state corresponds to the state with minimum energy and thus we can find it by minimizing

$$E[\psi] = \frac{\langle\psi|\widehat{H}|\psi\rangle}{\langle\psi|\psi\rangle}.$$

It could be convenient to introduce the concept of free energy, useful to search the equilibrium state of a system.
So taking $F = E - \mu N$, what we are searching is the condition of minimum free energy. Let us make some consideration.
First of all we introduce a normalization condition $\langle\psi|\psi\rangle = N$. Then we consider a mean field approximation, with $\psi(\vec{r}_1, ..., \vec{r}_N) = \psi(\vec{r}_1)\psi(\vec{r}_2)...\psi(\vec{r}_N)$, that means all particle in the same state.
What we obtain is $F[\psi] = \frac{\langle\psi|\widehat{H}-N\mu|\psi\rangle}{N}$, and applying the variational method we find

$$\begin{aligned}
\delta_\psi F[\psi] =& \frac{1}{N}\langle\delta\psi|\widehat{H} - N\mu|\psi\rangle \\
=& \frac{1}{N}\int \mathrm{d}^3\vec{r}^N \delta\psi^*(\vec{r})[\sum_{i=1}^{N}(-\frac{\hbar^2}{2m}\nabla_i^2 + U(\vec{r}_i)) - N\mu]\phi(\vec{r}) + \\
&+ \frac{1}{N}\int \mathrm{d}^3\vec{r}^N \delta\psi^*(\vec{r})[\int \mathrm{d}^3\vec{r'}^N V(\vec{r}, \vec{r'})|\psi(\vec{r'})|^2]\psi(\vec{r}) \\
=& \int \mathrm{d}^3\vec{r}\delta\psi^*(\vec{r})[-\frac{\hbar^2}{2m}\nabla^2 + U(\vec{r}) - \mu + \frac{(N-1)}{2}\int \mathrm{d}\vec{r'}V(\vec{r}, \vec{r'})|\psi(\vec{r'})|^2]\psi(\vec{r}) = 0.
\end{aligned}$$

This expression must be truth for each transformation $\delta\psi^*$, consequently we obtain

$$-\frac{\hbar^2}{2m}\nabla^2 + U(\vec{r}) + \frac{(N-1)}{2}\int \mathrm{d}\vec{r'}V(\vec{r}, \vec{r'})|\psi(\vec{r'})|^2]\psi(\vec{r}) = \mu\psi(\vec{r}).$$

If the bosons are weakly interacting [4], it is possible to substitute the true potential with the so called Fermi pseudo-potential approximation $V(\vec{r}, \vec{r'}) = V_0\delta(\vec{r} - \vec{r'})$, with $V_0 = \frac{4\pi\hbar^2}{m}a_S$ (a_S is the S-wave scattering length) and $\delta(\vec{r} - \vec{r'})$ the Dirac function

$$[-\frac{\hbar^2}{2m}\nabla^2 + U(\vec{r}) + \frac{(N-1)}{2}V_0|\psi(\vec{r})|^2]\psi(\vec{r}) = \mu\psi(\vec{r}),$$

that is the stationary Gross-Pitaevskii equation (GPE).
Using the variational method, it is possible to obtain also the time-dependent GPE. Minimizing the Dirac action

$$S = \int \mathrm{d}t \langle \psi(t) | i\hbar \frac{\partial}{\partial t} - \widehat{H} | \psi(t) \rangle, \tag{1.1}$$

we find the time-dependent GPE

$$i\hbar \frac{\partial}{\partial t}\psi(\vec{r},t) = [-\frac{\hbar^2}{2m}\nabla^2 + U(\vec{r}) + \frac{(N-1)}{2} g|\psi(\vec{r},t)|^2]\psi(\vec{r},t), \tag{1.2}$$

where $g = \frac{4\pi\hbar^2}{m} a_S$.

The trapping potential considered in our study is taken with a strong harmonic confinement in the yz plane, and with a double well potential on the x-axis

$$U(\vec{r}) = \frac{m_i \omega_i^2}{2}(y^2 + z^2) + V_{DW}(x) \tag{1.3}$$

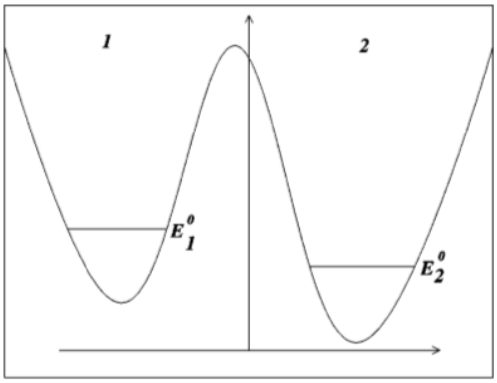

Figure 1.2: The monodimensional and asymmetric double-well potential V_{DW}

Coming back to Eq. (1.1), making explicit the trapping potential, we can find a monodimensional equation.
Let's consider the following ansalz [5]

$$\psi(\vec{r},t) = \frac{1}{\sqrt{\pi} a_\perp} e^{-\frac{y^2+z^2}{2a_\perp^2}} \Psi(x,t), \tag{1.4}$$

with $a_\perp = \sqrt{\frac{\hbar}{m\omega}}$ and $\int\int\int \mathrm{d}x\mathrm{d}y\mathrm{d}z|\psi(x,y,z)|^2 = N$.

Using Eqs. (1.3) and (1.4) in Eq. (1.1) we find

$$S = \int \mathrm{d}t \int \mathrm{d}\vec{r} \frac{1}{\pi a_\perp^2} e^{-\frac{y^2+z^2}{2a_\perp^2}} \Psi^*(x,t)[i\hbar\frac{\partial}{\partial t} + \frac{\hbar^2}{2m}\nabla^2 - \frac{m_i\omega_i^2}{2}(y^2+z^2) - \\ - V_{DW}(x) - \frac{g}{2}|\psi(\vec{r},t)|^2] e^{-\frac{y^2+z^2}{2a_\perp^2}} \Psi(x,t). \tag{1.5}$$

Here, introducing cylindrical coordinates, and integrating over ρ and θ we obtain

$$S = \int \mathrm{d}t \int \mathrm{d}x \Psi^*(x,t)[i\hbar\frac{\partial}{\partial t} + \frac{\hbar^2}{2m}\frac{d^2}{dx^2} - V_{DW}(x) - \epsilon - g_{1D}|\Psi(x,t)|^2]\Psi(x,t), \tag{1.6}$$

in which $\epsilon = \frac{\hbar^2}{2ma_\perp^2} + \frac{m\omega^2 a_\perp^2}{2}$ and $g_{1D} = \frac{g}{2\pi a_\perp^2}$.

Minimizing Eq. (1.6) respect to $\Psi^*(x,t)$, we get

$$i\hbar\frac{\partial}{\partial t}\Psi(x,t) = [-\frac{\hbar^2}{2m}\frac{d^2}{dx^2} + U_{DW}(x) + g_{1D}|\Psi(x,t)|^2]\Psi(x,t), \tag{1.7}$$

the 1-D GPE, where we have defined $U_{DW} = V_{DW} + \epsilon$.

Chapter 2

Bose-Einstein condensate in a double-well potential

What we consider in this chapter is a system of N bosons, confined in a double-well potential. Following the ansalz used by Smerzi in his work [6], wave functions localized in the right and left well can be seen as combinations of the first two eigenvectors of harmonic oscillator.
In particular

$$\phi_L(x) = \frac{1}{\sqrt{2}}(\Phi_0(x) - \Phi_1(x)),$$
$$\phi_R(x) = \frac{1}{\sqrt{2}}(\Phi_0(x) + \Phi_1(x)).$$

What we want to do now is to find the Josephson equations.
We start from 1-D GPE (1.7). $\Psi(x,t)$, given the two mode approximation, can be rewritten as follows

$$\Psi(x,t) = f_L(t)\phi_L(x) + f_R(t)\phi_R(x)$$

with

$$f_L(t) = \sqrt{N_L(t)}e^{i\theta_L(t)}$$
$$f_R(t) = \sqrt{N_R(t)}e^{i\theta_R(t)}.$$

Inserting the two-mode wavefunction in the (1.7), and multiplying the left-hand side by ϕ_R, we obtain:

$$i\hbar(\frac{\partial}{\partial t})[f_R \int |\phi_R|^2 \, dx + f_L \int \phi_R\phi_L dx] =$$

$$i\hbar(\frac{\partial}{\partial t})f_R = i\hbar(\frac{\dot{N_R}}{2N_R} + i\dot{\theta_R})f_R.$$

For the right-hand side, we obtain

$$\phi_R[-\frac{\hbar^2}{2m}\frac{d^2}{dx^2} + U_{DW}](f_L\phi_L + f_R\phi_R) +$$
$$+g_{1D}\int \phi_R \left|f(x,t)\right|^2 (f_L\phi_L + f_R\phi_R)dx.$$

Assuming $\phi_i = \phi_i^*$ (due to the definition of ϕ_i), the last term becomes

$$g_{1D} \int \phi_R \left| f(x,t) \right|^2 (f_L \phi_L + f_R \phi_R) dx =$$

$$g_{1D} \int \phi_R (f_L^* \phi_L + f_R^* \phi_R (f_L \phi_L + f_R \phi_R (f_L \phi_L + f_R \phi_R (x)) dx =$$

$$g_{1D} \int |\phi_R|^4 N_R f_R,$$

in which we neglect exponentially small $\phi_R \phi_L$ terms.
Rearranging we obtain

$$i\hbar(\frac{\dot{N_R}}{2N_R} + i\dot{\theta_R}) f_R = E_R f_R + K f_L + U N_R f_R, \tag{2.1}$$

with

$$E_R = \int \phi_R [-\frac{\hbar^2}{2m}\frac{d^2}{dx^2} + U_{DW}]\phi_R,$$
$$K = \int \phi_R [-\frac{\hbar^2}{2m}\frac{d^2}{dx^2} + U_{DW}]\phi_L,$$
$$U = g_{1D} \int |\phi_R|^4.$$

Now multiplying the left-hand side and the right-hand side by ϕ_L, we find:

$$i\hbar(\frac{\dot{N_L}}{2N_L} + i\dot{\theta_L}) f_L = E_L f_L + K f_R + U N_L f_L. \tag{2.2}$$

We set

$$z(t) = \frac{N_L - N_R}{N_0},$$
$$\theta(t) = \theta_R - \theta_L,$$

with $N_0 = N(0)$ the total number of particles at time t=0.

Summing Eq. (2.1) with its complex conjugate, and dividing by f_R, we get

$$-2\hbar\dot{\theta_R} = 2(E_R + U N_R + 2K\sqrt{\frac{N_L}{N_R}}\cos\theta). \tag{2.3}$$

We perform the same procedure for Eq. (2.2)

$$-2\hbar\dot{\theta_L} = 2(E_L + U N_L + 2K\sqrt{\frac{N_R}{N_L}}\cos\theta). \tag{2.4}$$

Subtracting Eq. (2.4) to Eq. (2.3)

$$\dot{\theta_R} - \dot{\theta_L} = \dot{\theta} = \frac{(E_L - E_R)}{\hbar} + \\ + \frac{U}{\hbar}(N_L - N_R) + \frac{2K}{\hbar}\frac{z}{\sqrt{1-z^2}}\cos(\theta),$$

and so

$$\dot{\theta} = \frac{\Delta E}{\hbar} + \frac{U}{\hbar} N_0 z + \frac{2K}{\hbar} \frac{z}{\sqrt{1-z^2}} \cos\theta, \tag{2.5}$$

with $\Delta E = (E_L - E_R)$ the difference between the energy in the two well, U the energy due to coupling effects and $2K$ the energy due to tunneling.

Now taking the difference between Eq. (2.1) and its complex conjugate, and dividing by $\frac{f_R}{N_R}$

$$i\hbar \dot{N_R} = +2iK\sqrt{N_L N_R}\sin\theta,$$

$$\dot{N_R} = +2\frac{K}{\hbar}\sqrt{N_L N_R}\sin\theta.$$

Doing the same for Eq. (2.2)

$$\dot{N_L} = -2\frac{K}{\hbar}\sqrt{N_L N_R}\sin\theta,$$

and consequently

$$\frac{\dot{N_L} - \dot{N_R}}{N_0} = \dot{z} = -2\frac{K}{\hbar}\sqrt{1-z^2}\sin\theta.$$

Finally, the Josephson equations for BEC are found:

$$\dot{\theta}(t) = \frac{\Delta E}{\hbar} + \frac{U}{\hbar} N_0 z + \frac{2K}{\hbar} \frac{z}{\sqrt{1-z^2}} \cos\theta, \tag{2.6}$$

$$\dot{z}(t) = -2\frac{K}{\hbar}\sqrt{1-z^2}\sin\theta. \tag{2.7}$$

Under the condition $\Delta E \neq 0$ and $U = 0$, Eqs. (2.6, 2.7) becomes

$$\dot{\theta}(t) = \frac{\Delta E}{\hbar},$$

$$\dot{z}(t) = -2\frac{K}{\hbar}\sin\theta,$$

and we get the "AC Josephson effect". In that case, in presence of a very small fractional imbalance ($|z| \ll 1, U|z| \ll K|z| \ll 1$, typical of superconductor), we find

$$\dot{\theta}(t) = \frac{\Delta E}{\hbar},$$

$$\dot{z}(t) = -2\frac{K}{\hbar}\sin\theta,$$

and introducing the Josephson current [7], defined as $I(t) = -\dot{z}(t)$, we obtain

$$I(t) = I(0)\sin(\theta_0 + \frac{\Delta E}{\hbar}t),$$

$$\dot{\theta}(t) = \frac{\Delta E}{\hbar},$$

that are the typical Josephson equations in superconductor.

Historically these were the first equations found by Josephson in 1962 [7]. The first Josephson junction was realized by Anderson and Rowell in 1963 [8] and they used two strips of superconductors separated by an insulator (Fig.(2.1)). In the following years it became clear that the role of superconductors could be replaced by ultracold gasses, giving thrust to the study of this important phenomenon. The first group to reach this result, using a BEC confined in a doublewell, was a research team from the university of Heidelberg in 2007 [9].

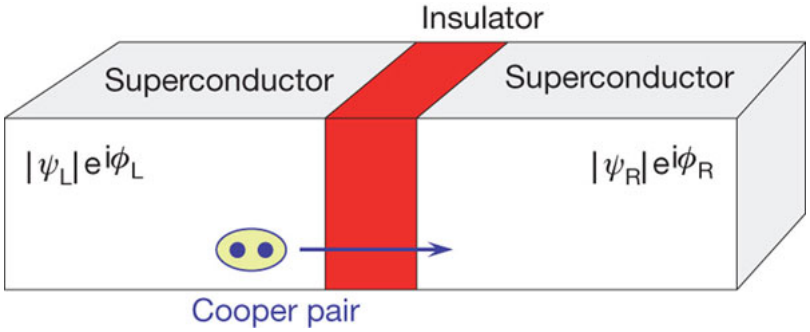

Figure 2.1: The Josephson junction is composed of two strips of superconductors separated by an insulator. The physics underlying the Josephson junction is based on tunnel effect, that allows the transition of Cooper pairs of electrons from one side to the other.

Now setting $\Delta E = 0$ and $z \ll 1$ we obtain

$$\dot{\theta}(t) = \frac{2K}{\hbar} z \cos\theta,$$

$$I(t) = -\dot{z}(t) = 2\frac{K}{\hbar} \sin\theta,$$

that describes the "DC Josephson effect". The effect is a direct current crossing the insulator in the absence of any external electromagnetic field, owing to tunneling. This DC Josephson current is proportional to the sine of the phase difference across the insulator, and may take values between $-I(0)$ and $I(0)$

Consequently what the Josephson effect underlines, is that taking a Josephson junction (Fig. 2.1), a current can flow through the junction without voltage across up to a maximum current $I(0) = I_c$, said critical current.

2.1 Computational analysis of different behaviors in BEC dynamics

First of all let us make a simplification.
We rewrite Eqs. (2.6, 2.7) as

$$\dot{\theta}(t') = \Delta E' + \Lambda z + \frac{z}{\sqrt{1-z^2}} \cos\theta, \tag{2.8}$$

$$\dot{z}(t') = -\sqrt{1-z^2} \sin\theta, \tag{2.9}$$

where we have rescaled to a dimensional time $\frac{t2K}{\hbar} \to t'$ and

$$\Delta E' = \frac{\Delta E}{2K}$$

$$\Lambda = \frac{UN_0}{2K}$$

Consequently the dimensionless parameters Λ and $\Delta E'$ determinate the dynamic regimes of the BEC tunneling. We also assume $\Lambda \geq 0$.
In particular it is possible to estimate the total, conserved energy:

$$H = \frac{\Lambda z^2}{2} + \Delta E' z - \sqrt{1 - z^2}\cos\theta, \tag{2.10}$$

and the equations of motion (2.8, 2.9) can be written in the Hamiltonian form

$$\dot{z} = -\frac{\partial H}{\partial \theta}$$
$$\dot{\theta} = \frac{\partial H}{\partial z}$$

2.1.1 The symmetric trap case $\Delta E = 0$

Rabi oscillations

For non interacting atoms ($\Lambda = 0$) the equations found describe sinusoidal Rabi oscillations between the two traps, with a frequency ω_R.
On a practical point of view, this behavior of the dynamics of the system could be used for important experimental observation [10].

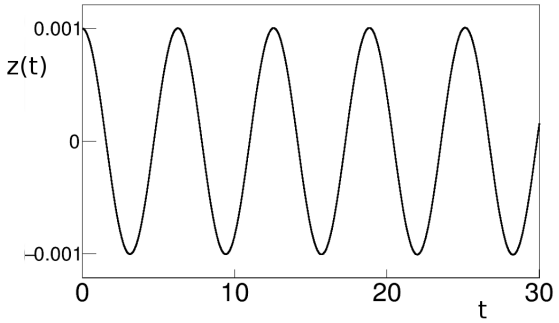

Figure 2.2: Rabi oscillations with Rabi frequency $\omega_R = (\frac{2}{\hbar})K$. Plot of the population imbalance $z(t)$ as a function of the rescaled time t', when the coupling energy $\Lambda = 0$ and for the specific initial condition $[z(0), \theta(0)]$=[0.001, 0].

Oscillations in zero-phase mode

In Fig. 2.3 we stressed out the different dynamics of population imbalance in different situations. Time t is expressed in units of $\frac{2K}{\hbar}$.

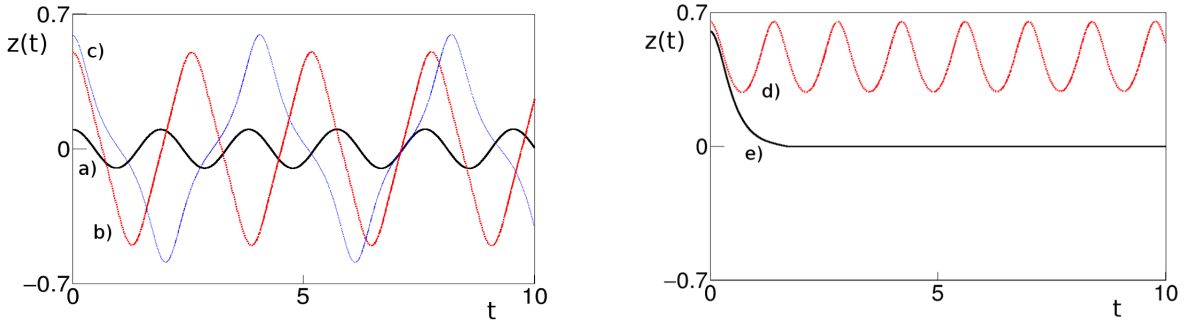

Figure 2.3: Population imbalance z(t) as a function of rescaled time t', when the coupling energy $\Lambda = 10$ and for the specific initial condition $\theta(0)$=0. We consider different values of the parameter $z(0)$: (a) $z(0) = 0.1$, (b) $z(0) = 0.5$, (c) $z(0) = 0.59$, (d) $z(0) = 0.65$, (e) $z(0) = 0.6$.

In particular we can see how, at fixed Λ, dynamics change drastically varying $z(0)$. With a small $z(0)$ (case a), we find sinusoidal oscillations. The period increases with $z(0)$ (case b), until arrive to not sinusoidal oscillations (case c). When $z(0)$ is equal to the critical value $z_c(0) = 0.6$ (case e), we find a transition from zero average oscillations (a, b, c) to a macroscopic quantum self-trapping (MQST) situation (d).
There are different ways in which this case can be obtain [6], but all of them correspond to the condition

$$H_0 = H(z(0), \theta(0)) = \frac{\Lambda}{2} z(0)^2 - \sqrt{1 - z(0)^2}\cos[\theta(0)] > 1.$$

Consequently the critical condition $H = 1$ leads to

$$\Lambda_c = 2\frac{1 + \sqrt{1 - z(0)^2}\cos[\theta(0)]}{z(0)^2}.$$

From this equation it is possible to find $z_c(0)$ fixing Λ.

Oscillations in π -phase mode

We now consider the tunneling dynamics in which $\langle\theta\rangle = \pi$. Fixing the value of $z(0) = 0.6$, we change Λ to analyze the different behaviors.

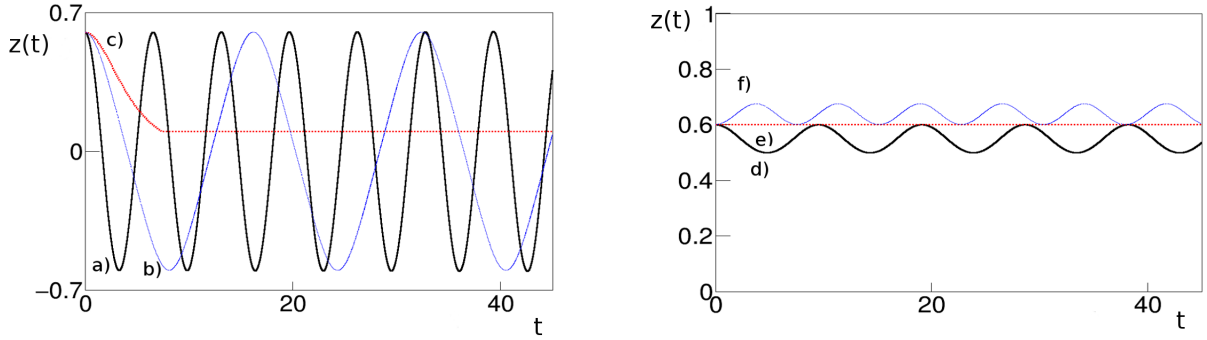

Figure 2.4: Population imbalance z(t) as a function of rescaled time t', for the specific initial condition $[z(0),\theta(0)]$=[0.6, pi]. We consider different values of the coupling energy Λ: (a) $\Lambda = 0.1$, (b) $\Lambda = 1.1$, (c) $\Lambda = 1.111$, (d) $\Lambda = 1.2$, (e) $\Lambda = 1.25$, (f) $\Lambda = 1.3$.

What we see, is that increasing Λ we obtain oscillation with an increasing period (cases a, b). Then, reaching the critical value $\Lambda_c = 2\frac{1+\sqrt{1-0.6^2}\cos[\pi]}{0.6^2} = 1.111$, we find the transition to MQST, just like the zero-phase mode.
But in that case we have different self-trapped behaviors (case d, f) and a stationary condition (case e).
Starting from Eq. (2.10), it's possible to find a class of degenerate GPE eigenstates that break the z-symmetry [6]:

$$\theta_s = (2n+1)\pi,$$

$$z_s^2 = 1 - \frac{1}{\Lambda^2},$$

and so $\Lambda_s = \frac{1}{\sqrt{1-z(0)^2}}$. These are stationary solutions for Eqs. (2.8, 2.9).
Consequently, when $\Lambda_c < \Lambda < \Lambda_s$ we have the first kind of MQST, when $\Lambda = \Lambda_s$ we have the stationary condition and when $\Lambda > \Lambda_s$ we have the second kind of MQST.
This behavior was impossible in the previous mode, due to the condition $\Lambda \geq 0$.

2.1.2 The asymmetric trap case $\Delta E \neq 0$

In this case we can find immediately two different situations.
If $\Delta E' \gg \Lambda z(0)$, we obtain something like the AC Josephson effect, with approximated equations:

$$\dot{\theta}(t') \approx \Delta E',$$

$$\dot{z}(t') = -\sin\theta.$$

This implies a small oscillation of population imbalance with a well defined frequency $\omega_0 = \Delta E'$. It is showed in Fig. (2.5). We can easily see that this is a nonzero average oscillation.

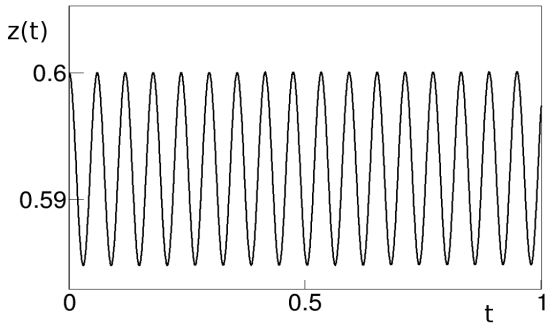

Figure 2.5: Population imbalance z(t) as a function of rescaled time t', for the specific initial condition $[z(0),\theta(0)]$=[0.6, 0]. We set the coupling energy $\Lambda = 10$ and the nergy difference $\Delta E' = 100$.

If instead $\Delta E' \ll \Lambda z(0)$ we find similar results to the symmetric trap case, with some difference. The introduction of $\Delta E'$ changes the hamiltonian, that becomes

$$H = \frac{\Lambda z^2}{2} + \Delta E' z - \sqrt{1 - z^2}\cos\theta.$$

This brings to new Λ_c and Λ_s values. In Fig.(2.6) we give an important example of the difference between the two trap cases.

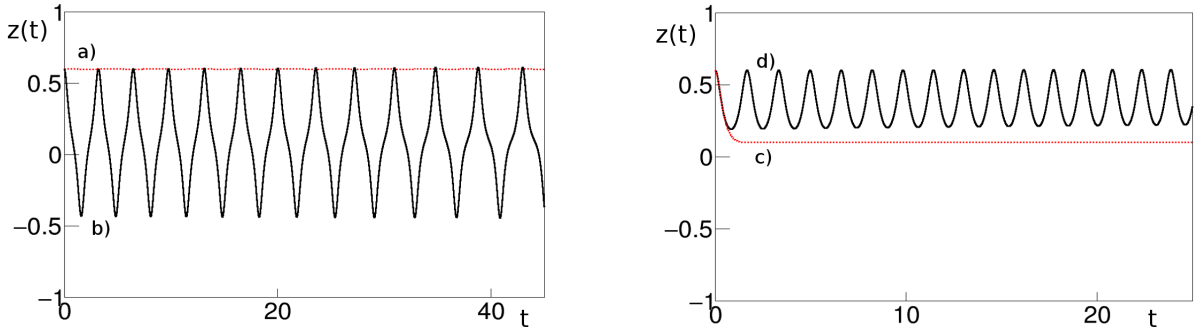

Figure 2.6: Population imbalance z(t) as a function of rescaled time t', with energy difference $\Delta E' = -1.2$ and for the specific initial condition $[z(0),\theta(0)]$=[0.6, 0]. We consider different values of the coupling energy Λ: (a) $\Lambda = 0.1$, (b) $\Lambda = 1.1$, (c) $\Lambda = 1.111$, (d) $\Lambda = 1.2$, (e) $\Lambda = 1.25$, (f) $\Lambda = 1.3$.

First of all, what we expect to see is the presence of a new Λ_c, obtainable from the MQST condition $H = 1$. In this specific case the theoretical value is $\Lambda_c^t = 14$, but the experimental one is $\Lambda_c^r = 13.64$. That means that $\Delta E'$ changes the MQST condition.
Then we see that is possible to find, with some particular negative values of $\Delta E'$, a positive Λ_s also in the zero-phase mode. That implies the presence of a stationary condition.
The last important thing to stress is that the nonzero average imbalance persist, and its value depend on Λ and $\Delta E'$.

Chapter 3

From dissipative GPE to dissipative Josephson Equations

Until now we consider the dynamics of a BEC in a double-well confinement in a conservative system, using a GPE to describe it. But an important role in these processes is linked to the dissipation that is always present, and affects the dynamics of the junction, thereby changing the tunneling process. A way to take into account this effects is adding a dissipative term in Eq. (1.7) we obtain the "dissipative 1D GPE equation"

$$i\hbar(\frac{\partial}{\partial t}+\gamma)\Psi(x,t)=[-\frac{\hbar^2}{2m}\frac{d^2}{dx^2}+U_{DW}(x)+g\left|\Psi(x,t)\right|^2]\Psi(x,t), \tag{3.1}$$

where γ is the dissipative coefficient.
Doing the same mathematical steps of chapter 2, we find

$$i\hbar(\frac{\dot{N_L}}{2N_L}+i\dot{\theta_L}+\gamma)f_L=E_Lf_L+Kf_R+UN_Lf_L$$

$$i\hbar(\frac{\dot{N_R}}{2N_R}+i\dot{\theta_R}+\gamma)f_R=E_Rf_R+Kf_L+UN_Rf_R$$

and consequently

$$\dot{\theta}_R=-\frac{1}{\hbar}(E_R+UN_R+2K\sqrt{\frac{N_L}{N_R}}\cos\theta),$$

$$\dot{\theta}_L=-\frac{1}{\hbar}(E_L+UN_L+2K\sqrt{\frac{N_R}{N_L}}\cos\theta),$$

$$\dot{N_R}=-2\gamma N_R+2\frac{K}{\hbar}\sqrt{N_LN_R}\sin\theta,$$

$$\dot{N_L}=-2\gamma N_L-2\frac{K}{\hbar}\sqrt{N_LN_R}\sin\theta.$$

Setting

$$z(t)=\frac{N_L-N_R}{N_0},$$

$$\eta(t)=\frac{N_L+N_R}{N_0},$$

$$\theta(t) = \theta_R - \theta_L,$$

with $N_0 = N(0)$ the total number of particles at time t=0, we get

$$\dot{\theta}(t) = \frac{\Delta E}{\hbar} + \frac{U}{\hbar} N_0 z(t) + \frac{2K}{\hbar} \frac{z(t)}{\sqrt{\eta(t)^2 - z(t)^2}} \cos\theta(t), \tag{3.2}$$

$$\dot{z}(t) = -2\gamma z(t) - \frac{2K}{\hbar} \sqrt{\eta(t)^2 - z(t)^2} \sin\theta(t), \tag{3.3}$$

$$\dot{\eta}(t) = -2\gamma\eta(t). \tag{3.4}$$

The difference between Eqs. (2.6, 2.7) and Eqs.(3.2, 3.3, 3.4) are:

a) In the population imbalance's time derivative there is a new term due to the presence of γ. This one is linked with a dissipative behavior of the equation of motion for z. Taking the derivative of Eq.(3.3) with respect to t we find

$$\ddot{z} = -2\gamma\dot{z} - \frac{\partial}{\partial t}\left(\frac{2K}{\hbar} \sqrt{\eta(t)^2 - z(t)^2} \sin\left(\theta(t)\right)\right),$$

and clearly the new term adds a dissipative trend in the dynamics.

b) There is the introduction of a new variable, η, that can be interpreted as the BEC fraction. Consequently Eq. (3.4) implies that the number of condensated bosons changes in time. In this particular case we find that the BEC fraction has a negative exponential trend $\eta(t) = e^{-2\gamma t}$ with $\eta(0) = 1$.

3.1 Computational analysis

As we have already said, the introduction of γ leads to a dissipative effect. Let us figure it with the computational analysis. Taking some example from chapter 2.1 it is possible to point out the role of γ in the dynamics.

Before starting, it is useful to introduce $\Gamma = 2\gamma\frac{\hbar}{2K}$, to find the rescaled equation $\dot{z}(t) = -\Gamma z(t) - \sqrt{\eta(t)^2 - z(t)^2}\sin\left(\theta(t)\right)$.

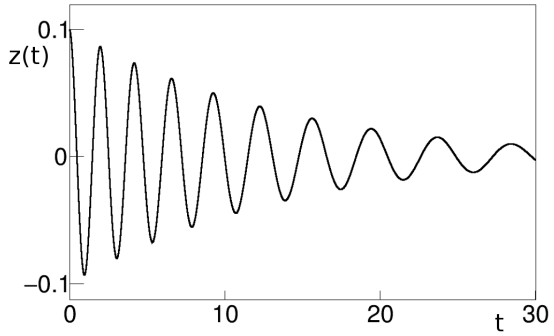

Figure 3.1: Population imbalance z(t) as a function of rescaled time t', where the coupling energy $\Lambda = 10$, $\Delta E' = 0$, the dissipative term $\Gamma = 0.05$ and for the specific initial condition $[z(0),\theta(0)]=[0.1, 0]$.

In Fig. (3.1) it is clear that, in general, the oscillation regime is affected by a continuous reduction in the amplitude, due to the presence of the dissipative term.

Now studying how the limit case of Fig. (2.3, e) change with the introduction of Γ, we find that there is not anymore a well defined condition for the transition from the MQST regime to the zero average oscillation regime.

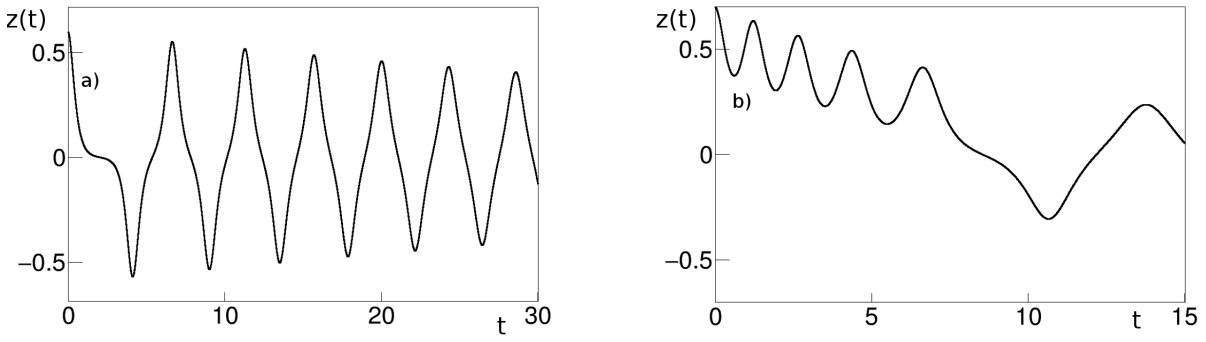

Figure 3.2: Oscillation of z(t) as a function of rescaled time t', where the coupling energy $\Lambda = 10$, $\Delta E' = 0$, and for initial condition $\theta(0) = 0$. We consider different values of[$z(0)$,Γ]: (a) [0.6, 0.01], (b) [0.7, 0.1].

Watching Fig. (3.2, a) it is clear that the presence of Γ introduces a time-dependent changing of behavior. Furthermore Fig. (3.2, b) give us an idea of what a big Γ does to an initial MQST regime.

The last thing to consider is the stationary condition, and the near MQST behaviors, found in the π-phase mode.

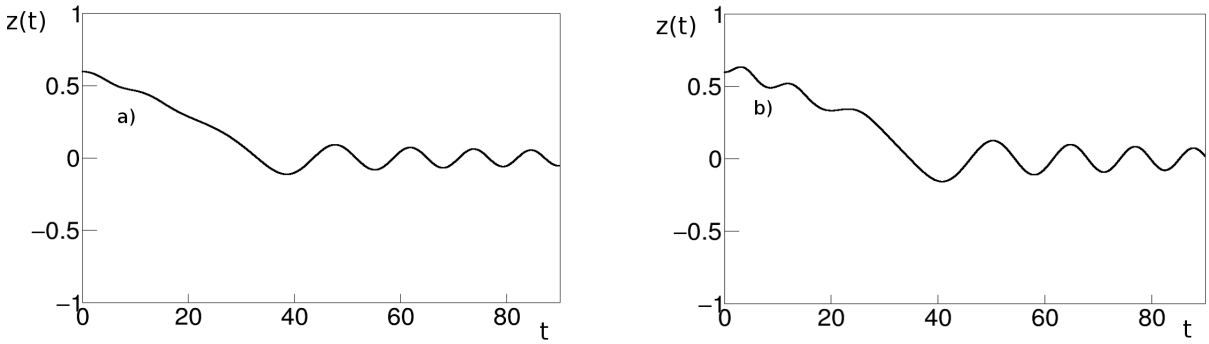

Figure 3.3: Oscillation of z(t) as a function of rescaled time t', where the energy difference $\Delta E' = 0$, the dissipative term $\Gamma = 0.004$, and for initial condition $[z(0), \theta(0) = \pi]$. We consider different values of Λ: (a) $\Lambda = 1.25$, (b) $\Lambda = 1.3$.

Fig.(3.3) show that now it is not possible to have a stationary condition, and show that the presence of Γ not only changes the amplitude of the oscillation, but also its average, $\langle z \rangle$, from the starting value to zero.

Chapter 4

Experimental evidence of Josephson effects

As already said in chapter 2, the first experimental evidence of Josephson effect was with Anderson and Rowell in 1963 [8], studying a Josephson junction with superconductors. Only in the first years of this decade they were made experiments concerning with ultracold gasses.

In Fig. (4.1) is reported what the research team from the university of Heidelberg [9] found about dynamics of the system.

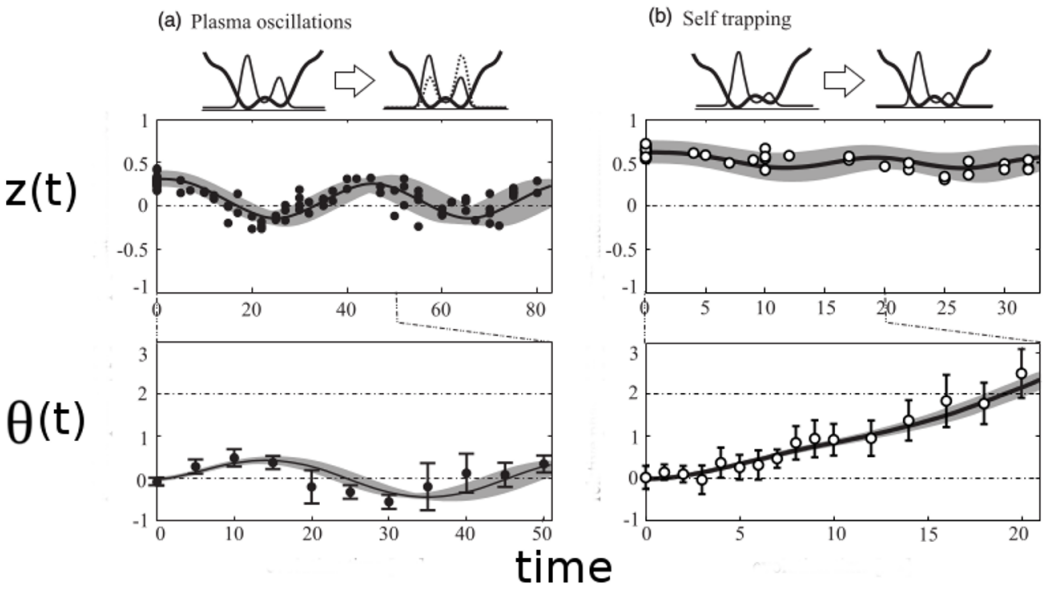

Figure 4.1: Dynamical response of the bosonic Josephson junction. Column (a) shows the measurement of temporal evolution of population imbalance $z(t)$ and phase difference $\theta(t)$ in the Josephson regime. Column (b) shows the measurement of temporal evolution of population imbalance $z(t)$ and phase difference $\theta(t)$ in the self-trapping regime.

We can clearly seen the presence of two types of regimes, just as we found: the Josephson regime, with zero average oscillations, and the MQST regime, in which the

population imbalance is locked. This work doesn't show the existent of dissipative effects. But it is possible to find evidence of these in a recent study, by Barzanjeh and Vitali [11].

This work shows that the coupling between two non linear nanomechanical resonators (NMRs) has some interesting analogies with Josephson Junction. In their work, they observe that Eqs. (2.6, 2.7) describe very well the dynamics of two coupled NMRs. Looking Fig. (4.2) we can see that they get the same dynamical result obtained in chapter 2, in which g is our Λ, g_{cr} is Λ_c and g_s is Λ_s .
Subsequently they include the effect of mechanical damping, by adding phonon loss terms γ in the Hamiltonian of the system, finding Eqs. (3.2, 3.3, 3.4), and so obtaining the same dissipative dynamics of chapter 3 (Fig. 4.3).

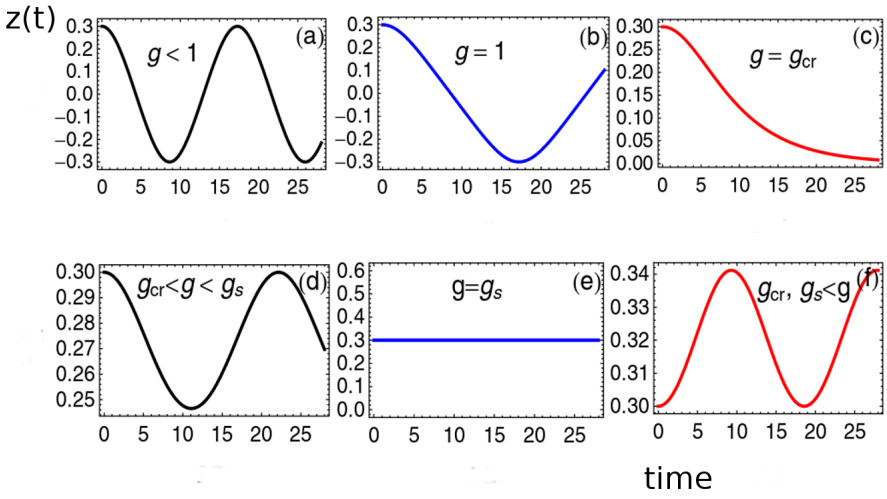

Figure 4.2: Population imbalance as a function of rescaled time, in the conservative case. Initial condition: $z(0) = 0.3$, $\theta(0) = \pi$, $\Delta E = 0$. The coupling energy is g. Figures (a) and (b) represent oscillations for small value of g. Increasing g the period grows. Figure (c) shows the limit case in which g reaches the critical value for the regime changing. Figures (d) and (f) show the two self-trapping oscillations with different mean values. In the end figure (e) shows the stationary case.

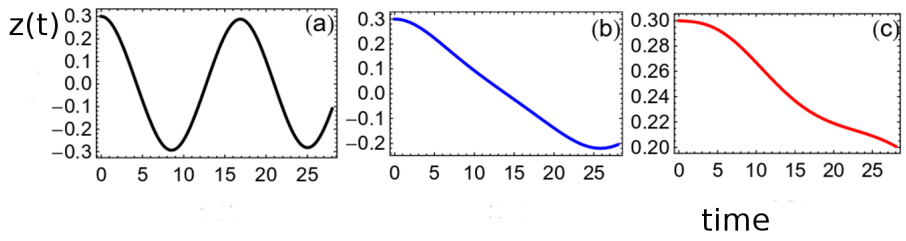

Figure 4.3: Population imbalance $z(t)$ as a function of rescaled time, in the dissipative case. Initial condition: $z(0) = 0.3$, $\theta(0) = \pi$, $\gamma = 0.001$, $\Delta E = 0$. Figure (a) shows the damping of oscillations for small values of the coupling energy. Figure (b) displays the limit case for the regime changing and figure (c) exhibits the stationary case. In all cases $z(t)$ goes to zero

Coming back to the Josephson junction case, the effect of mechanical dumping is replaced by the creation of quantum vortex. For example, a research team from the University of Maryland [12], have experimentally measured transport of superfluid bosonic atoms in a mesoscopic system. They observe the presence of a large dissipation, related to the creation of excitations in one of the reservoir. They modeled this dissipation with vortex pair production by a mechanism considered by Feynmann [13].
To fit the behaviour found, they model their system as a RLC circuit (Fig. 4.4), where the capacitor represents the energy stored in the two reservoirs of BEC, the inductor represents kinetic energy stored in the flow of atoms, and the resistor in parallel allows additional current to flow in the Josephson junction, but with dissipation.

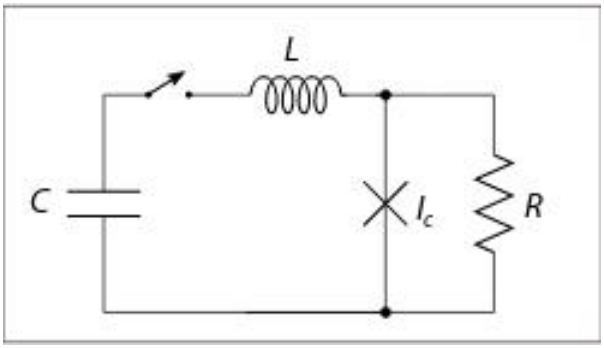

Figure 4.4: A circuit composed by a Josephson junction connected in series with an inductance L and a capacitance C, and connected in parallel with a resistance R.

The equations that describe the circuit in Fig. (4.4) are

$$-\dot{z} = I = I_R + I_{JS} \tag{4.1}$$

$$\dot{\theta} = R(I - I_C \sin\theta) \tag{4.2}$$

$$\dot{I} = -\frac{1}{L}(-\frac{z}{C} + R(I - I_C \sin\theta)) = -\frac{1}{L}(-\frac{z}{C} + \dot{\theta}) \tag{4.3}$$

Comparing this with what we found, we get that, just like for Eq. (3.3), even in Eq. (4.1) appear an additional term not present in the classical Josephson equation Eq. (2.7). In that case it is linked with the presence of resistance R in the circuit.

Conclusion

We have investigated the Josephson junction dynamics with a Bose-Einstein condensate under double-well confinement both without and with dissipation. Using a two-mode model, we have described the temporal oscillations of the population imbalance of the condensates. Our predictions show how the behaviour of the dynamics changes, from Josephson regime to self-trapping regime, varying system's parameters: the coupling energy, the tunneling effect and the energy difference between the two wells. We clarify the connection and the difference of the two different regimes in the conservative and dissipative situation, through a numerical analysis made using a four-order Runge-Kutta method. What we found is that, in the conservative case, the initial condition define a specific regime. We saw that varying the coupling energy it is possible to modify the period of the oscillations, and varying the energy difference between wells it is possible to change the average of the oscillations. Instead, in the dissipative case, the population imbalance goes to zero, faster the greater is the dissipative term. So in this situation it is impossible to have a self-trapping regime.

The interest in this research has been borne out by the possibility that experimental realization of weakly coupled Bose-Einstein condensates might add new tool to quantum optics with interacting matter waves. Moreover, the study of the self-trapping phenomenon could provide a test of the validity of the mean field description in atomic gases in the strong nonlinear regime [14].

Appendix A

Discussion about programs used in computational analysis

For the computational analysis, the algorithm used for the approximation of solutions of ODEs was the 4-order Runge-Kutta method, that is the widely used. This is a method that use a particular discretization of the time-depending variables to approximate the solutions. Taking the following initial value problem

$$\dot{y} = f(t, y)$$

$$y_0 = y(t_0)$$

we pick a step-size $h > 0$ and we use this discretization:

$$y_{n+1} = y_n + \frac{h}{6}(k_1 + 2K_2 + 2k_3 + k_4)$$

$$t_{n+1} = t_n + h$$

with

$$\begin{aligned} k_1 &= f(t_n, y_n) \\ k_2 &= f(t_n + \frac{h}{2}, y_n + \frac{h}{2}k_1) \\ k_3 &= f(t_n + \frac{h}{2}, y_n + \frac{h}{2}k_2) \\ k_4 &= f(t_n + h, y_n + hk_3) \end{aligned}$$

k_1 is the increment based on the slope at the beginning of the interval, using y (Euler's method);
k_2 is the increment based on the slope at the midpoint of the interval, using $y + \frac{h}{2}k_1$;
k_3 is again the increment based on the slope at the midpoint, but now using $y + \frac{h}{2}k_2$;
k_4 is the increment based on the slope at the end of the interval, using $y + hk_3$.
The RK4 method is a fourth-order method, meaning that the local truncation error is on the order of $O(h^5)$, while the total accumulated error is on the order of $O(h^4)$.

To produce graphics, and so to complete the analysis, we write a Macro for the program ROOT.

ROOT is a modular scientific software framework, made by CERN. It provides all the functionalities needed to deal with big data processing, statistical analysis, visualization and storage. It is mainly written in C++. With this Macro we was able to find the step by step solutions of ODEs, using the RK4 method aforementioned, and to report them on graphics, showing the time evolution of the solutions.

References

[1] S.N. Bose. *Zeitschrift fur Physik*, **26**:178, 1924.

[2] A. Einstein. *Sitzungsberichte der Preussischen Akademie der Wissenschaften*, **1**:3, 1925.

[3] M.H. Anderson, J.R. Ensher, M.R. Matthews, C.E. Wieman, and E.A. Cornell. *Science*, **269**:198, 1995.

[4] L. Salasnich, A. Parola, and L. Reatto. *Phys. Rev. A*, **57**:R3180, 1998.

[5] L. Salasnich and B.A. Malomed. *Phys. Rev. A*, **74**:053610, 2006.

[6] A. Smerzi, S. Raghavan, S. Fantoni, and S.R. Shenoy. *Phys. Rev. A*, **59**:620, 1999.

[7] B.D. Josephson. *Physics Letters*, **1**:241, 1962.

[8] P.W. Anderson and J.M. Rowell. *Phys. Rev. Lett.*, **10**:230, 1963.

[9] R. Gati and M. K. Oberthaler. *J. Phys. B: At. Mol. Opt. Phys.*, **40**:R61, 2007.

[10] S. Inouye, M.R. Anfrews, J. Stenger, H.J. Miesner, D.M. Stamper-Kurn, and W. Ketterle. *Nature*, **392**:151, 1998.

[11] S. Barzanjeh and D. Vitali. *Phys. Rev. A*, **93**:033846, 2016.

[12] J.G. Lee, S. Eckel, F. Jendrzejewski, C.J. Lobb, G.K. Campbell, and W.T. Hill. *Phys. Rev. A*, **93**:063619, 2016.

[13] R.P. Feynmann. *Prog. Low Temp. Phys*, **2**:17, 1955.

[14] A.I. Streltsov, L.S. Cederbaum, and N. Moiseyev. *Phys. Rev. A*, **70**:053607, 2004.